# Role of Electronic Structure in the Martensitic Phase Transition of $Ni_2Mn_{1+x}Sn_{1-x}$ Studied by Hard-X-Ray Photoelectron Spectroscopy and *Ab Initio* Calculation

M. Ye,[1] A. Kimura,[1,*] Y. Miura,[2] M. Shirai,[2] Y. T. Cui,[3] K. Shimada,[3] H. Namatame,[3] M. Taniguchi,[1,3] S. Ueda,[4] K. Kobayashi,[4] R. Kainuma,[5] T. Shishido,[6] K. Fukushima,[7] and T. Kanomata[7]

[1]*Graduate School of Science, Hiroshima University, 1-3-1 Kagamiyama, Higashi-Hiroshima, 739-8526, Japan*
[2]*Research Institute of Electrical Communication, Tohoku University, Sendai 980-8577, Japan*
[3]*Hiroshima Synchrotron Radiation Center, Hiroshima University, 2-313 Kagamiyama, Higashi-Hiroshima, 739-0046, Japan*
[4]*NIMS Beamline Station at SPring-8, National Institute for Materials Science, Sayo, Hyogo 679-5148, Japan*
[5]*Institute for Multidisciplinary Research for Advanced Materials, Tohoku University, Sendai 980-8577, Japan*
[6]*Institute for Materials Research, Tohoku University, Sendai 980-8577, Japan*
[7]*Faculty of Engineering, Tohoku Gakuin University, Tagajo, Miyagi 985-8537, Japan*

(Received 10 February 2010; published 26 April 2010)

We have revealed the underlying mechanism of the martensitic phase transition (MPT) in a new class of ferromagnetic shape memory alloys, $Ni_2Mn_{1+x}Sn_{1-x}$, by the combination of bulk-sensitive hard-x-ray photoelectron spectroscopy and a first-principles density-functional calculation. The Ni 3*d* $e_g$ state in the cubic phase systematically shifts towards the Fermi energy with an increase in the number of Mn atoms substituted in the Sn sites. An abrupt decrease of the intensity of the Ni 3*d* $e_g$ states upon MPT for $x = 0.36$–$0.42$ has been observed in the vicinity of the Fermi level. The energy shift of the Ni 3*d* minority-spin $e_g$ state in the cubic phase originates from hybridization with the antiferromagnetically coupled Mn in the Sn site. Below the MPT temperature, the Ni 3*d* state splits into two levels located below and above the Fermi energy in order to achieve an energetically stable state.

DOI: 10.1103/PhysRevLett.104.176401 PACS numbers: 71.15.−m, 81.30.Kf, 71.20.−b, 79.60.−i

Since ferromagnetic Ni-Mn-Ga [1] was proposed as a new type of shape memory alloy (SMA) showing a large magnetic field-induced strain (MFIS) in 1996 [2], this kind of SMA has attracted considerable attention as a magnetic actuator material [3,4]. This MFIS is due to a rearrangement of martensite variants by an external magnetic field induced by a strong coupling between magnetic and mechanical variables. Recent reports have shown that Ni-Mn-In, Ni-Mn-Sn, and Ni-Mn-Sb alloy systems are different types of magnetic SMAs, undergoing a martensitic phase transition (MPT) from the cubic Heusler $L2_1$ structure to the layered structure where, noticeably, the magnetization in the martensite phase of this system is significantly smaller than that in the austenite one [5]. Furthermore, in Co-doped Ni-Mn-In alloys a magnetic-field-induced phase transition (MFIT) from a weak-magnetic martensite to a ferromagnetic austenite phase at 298 K has been reported and a shape recovery of about 3% due to the MFIT has been confirmed for a predeformed single crystal [6]. This attractive property could enable one to obtain an extremely large stress of over 100 MPa that is several decades larger than that generated in the conventional ferromagnetic SMAs [6,7]. In addition, this group of alloys shows many other interesting properties, such as an inverse magnetocaloric effect [8], a giant magnetoresistance effect [9], giant magnetothermal conductivity [10], and an exchange bias effect [11].

Macroscopic measurements have been carried out mainly for Ni-Mn-Sn alloys with 50% Ni. It has been reported that the MPT from the ferromagnetic austenite phase is observed in the temperature range of 100–230 K for $Ni_2Mn_{1+x}Sn_{1-x}$ ($0.36 \leq x \leq 0.46$) [5,8] and that the crystal structures of austenite and martensite phases for $Ni_2Mn_{1.44}Sn_{0.56}$ are a Heusler-type cubic structure and an orthorhombic four-layered ($4O$) structure, respectively [5,12]. The magnetic properties of the austenite phase for the Ni-Mn-Sn alloy have been reported by Brown *et al.* [12]. Very recently, the magnetic behavior of the martensite phase in the $Ni_2Mn_{1.46}Sn_{0.52}(^{57}Fe_{0.02})$ alloy has been determined by Mössbauer spectroscopy as being paramagnetic [13]. According to a recent neutron diffraction experiment, the magnetic correlations are antiferromagnetic in the martensite phase, whereas they are ferromagnetic in the austenite phase even in the temperature range well above the Curie temperature [14]. It is important to note that the electrical resistivity in the martensite phase of the Ni-Mn-Sn alloys is around 2 times larger than that in the austenite phase [15] and that its thermoelectric properties are affected by the MPT [16]. This behavior suggests that the density of states in the vicinity of the Fermi energy drastically changes upon the MPT. Thus, although the Ni-Mn-Sn alloys show very interesting physical behaviors, the origin of them is still under discussion.

Most of the theoretical explanations concerning the underlying mechanism of MPT have been phenomenological studies based on the free energy expansion [4]. Some first-principles calculations, especially on Ni-Mn-Ga systems, have provided different interpretations on the origin of MPT, such as a Jahn-Teller distortion [17] and Fermi

 

surface nesting [18]. Furthermore, no decisive explanation has been provided for the question of why MPT occurs only in the off-stoichiometric condition for Ni-Mn-Z alloys.

Here we have clarified the origin of MPT from the electronic structure point of view for $Ni_2Mn_{1+x}Sn_{1-x}$ in the off-stoichiometric condition by hard-x-ray photoelectron spectroscopy and a state-of-the-art first-principles calculation.

Experimentally, the polycrystalline $Ni_2Mn_{1+x}Sn_{1-x}$ ($0 \leq x \leq 0.42$) were prepared by the procedure described elsewhere [19]. The structural refinement of $Ni_2Mn_{1+x}Sn_{1-x}$ ($0 \leq x \leq 0.42$) was carried out by the x-ray powder diffraction data using the standard Rietvelt technique. All the samples were shown to crystallize in the $L2_1$ structure at room temperature. Furthermore, it was confirmed that the excess Mn atoms on $Ni_2Mn_{1+x}Sn_{1-x}$ ($0 \leq x \leq 0.42$) occupy the vacant Sn sites. This is consistent with the results reported earlier [12,20]. We used photoelectron spectroscopy to thoroughly probe the change of valence electronic structures of the $x = 0.42$, 0.40, and 0.36 compounds, whose starting temperatures of MPT ($M_s$) range from 230 to 80 K. By using photon energy of 6 keV, mean free path of photoelectrons excited from the valence band reaches as deep as ~5 nm, where the surface contribution is well suppressed [21]. The total energy resolution of the spectra was set to 240 meV. All of the measurements were performed in ultrahigh vacuum (better than $5 \times 10^{-7}$ Pa). Contaminant-free sample surfaces were obtained by *in situ* fracturing.

Figures 1(a) and 1(b) illustrate the valence band photoelectron spectra for $x = 0.42$ and 0.36 at several different temperatures, in which the samples experienced the MPT by cooling down. A peak located around a binding energy ($E_B$) of 1.5 eV was observed that did not obviously change in all of the samples over the whole measured temperature range. Moreover, in the vicinity of the Fermi energy ($E_F$), a sharp peak was observed at $E_B = 0.3$–0.4 eV at 300 K ($T \geq M_s$) in the austenite phase with the cubic Heusler $L2_1$ lattice structure. A sharp peak at a similar binding energy near $E_F$ has also been reported for $Ni_2MnGa$ [18], which is attributed to the Ni $3d$ $e_g$ minority-spin states. In Fig. 1(a), the photoelectron spectra of $Ni_2Mn_{1.42}Sn_{0.58}$ ($x = 0.42$) are exhibited for temperatures from 300 to 160 K. The sharp peak ($E_B = 0.3$ eV) near $E_F$, as well as the prominent peak at 1.5 eV, remains unchanged till 240 K, a temperature at which the material is still in its austenite phase. A sudden reduction of the peak near $E_F$ is clearly observed when the temperature is decreased from 240 to 220 K across the MPT temperature (230 K), while the peak at 1.5 eV remains unchanged. When the sample temperature is further decreased down to 160 K, no change in either structure has been observed, indicating that the electronic and lattice structures have been stabilized in the martensite phase.

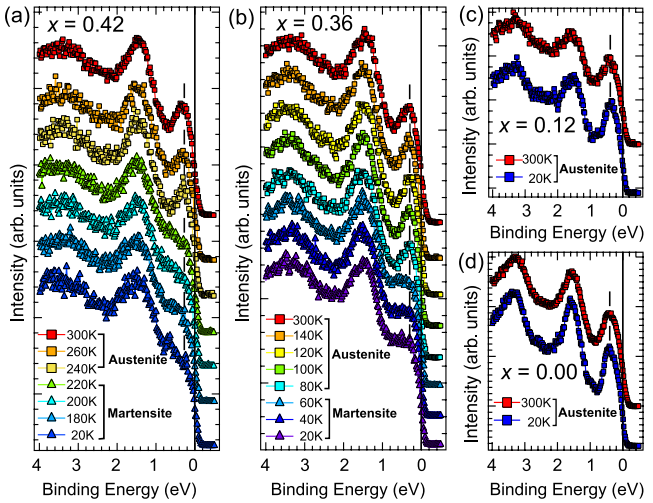


FIG. 1 (color online). (a)–(d) Valence-band spectra of $Ni_2Mn_{1+x}Sn_{1-x}$ with $x = 0.42$, 0.36, 0.12, and 0.00, acquired by hard-x-ray photoelectron spectroscopy ($h\nu = 5956.5$ eV) at several temperatures. The Fermi energy is taken as the origin of binding energy.

As for the samples with $x = 0.40$ (not shown) and 0.36, with $M_s = 190$ and 80 K, respectively, similar changes in the valence electronic structure were observed, as shown in Fig. 1(b) for $x = 0.36$. An abrupt intensity drop of the peak near $E_F$ was also found in these samples. In order to further confirm the relationship between the change of valence electronic structure and MPT, two additional samples with lower concentrations ($x = 0.12$ and 0.00) that do not show a MPT were measured with a similar procedure. As illustrated in Figs. 1(c) and 1(d), no noticeable change near $E_F$ is observed between 300 and 20 K for both samples, except for a slight change due to thermal broadening, which can be regarded as evidence for the direct relationship between the intensity drop in the valence density of states (DOS) and the MPT process.

The temperature-dependent spectra of the samples shown in Figs. 1(a) and 1(b) suggest that there is a close relationship between the density of states near $E_F$ and the occurrence of MPT in the ferromagnetic states and illustrate the important role of electronic structure in producing lattice deformations.

To gain further insight into the origin of the MPT observed in the ferromagnetic state of $Ni_2Mn_{1+x}Sn_{1-x}$, we have investigated the energy position of the peak near $E_F$, which is apparently responsible for the MPT, over a range of stoichiometry. Figure 2(a) shows the valence-band spectra in the austenite phase (300 K) for $x = 0.00$–0.42. Here, the systematic energy shift of the peak towards $E_F$ can be observed with increasing $x$. It is noticeable that for $x = 0.00$ and 0.12 the positions of this peak are located far away from the $E_F$ compared to those accompanying MPT. Thus, it should be reasonable to attribute the approaching

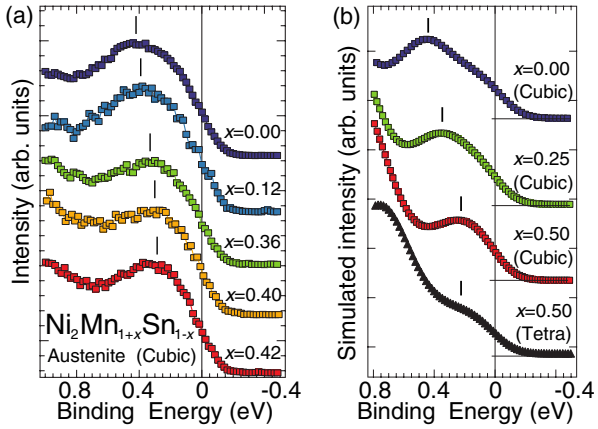


FIG. 2 (color online). (a) Valence-band spectra of $Ni_2Mn_{1+x}Sn_{1-x}$ with various $x$'s in cubic Heusler $L2_1$ phase (300 K). (b) The simulated spin-integrated x-ray photoelectron spectra.

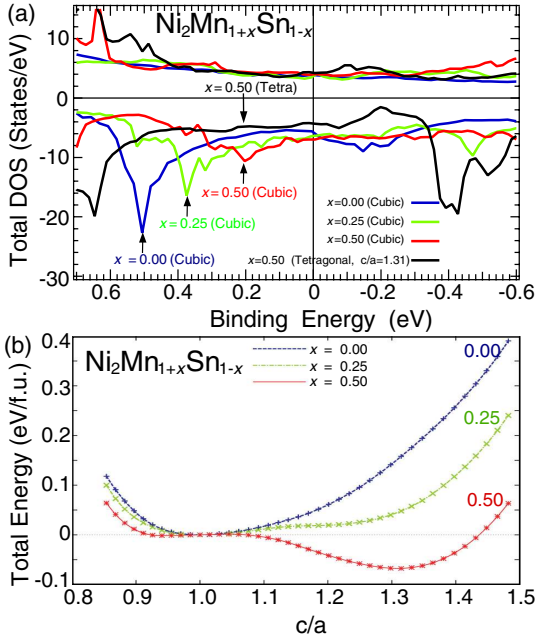


FIG. 3 (color online). (a) The total density of states (DOS) near $E_F$, in the cubic (austenite) phase of $Ni_2Mn_{1+x}Sn_{1-x}$ for $x = 0$ , 0.25, and 0.5, respectively. The DOS in the tetragonal phase ($c/a = 1.31$) for $x = 0.5$ is also shown for comparison. (b) The total energy difference (per formula unit) relative to the cubic phase as a function of the axial ratio, $c/a$, in the tetragonal structure calculated for $Ni_2Mn_{1+x}Sn_{1-x}$ with $x = 0$, 0.25, and 0.5, respectively.

of this peak towards $E_F$ as an important factor that triggers the occurrence of MPT in the ferromagnetic states.

Nevertheless, this experimental fact seems to disagree with the prediction of a pure rigid band model; by simply considering the number of valence electrons (NVE), we would expect the larger NVE of Mn than Sn to result in a rise of $E_F$ if the Sn site is substituted by a Mn atom. The abnormal shift of the peak in the vicinity of $E_F$, which plays an important role in the MPT, suggests that the mechanism of the Mn-substitution effect should be further investigated.

In order to elucidate the role of excess Mn atoms in the MPT of the Ni-Mn-Sn alloys, we have carried out first-principles density-functional calculations. The VIENNA *ab initio* simulation package [22,23] was used for the first-principles calculations. The spin-polarized generalized gradient approximation [24] is adopted for the exchange and correlation energies. The atomic core potential is described by the projector augmented wave method [25,26]. The lattice constant $a$ in the cubic phase is relaxed so as to minimize the total energy for each composition. The lattice constant thus obtained decreases from 6.060 Å ($x = 0$) to 5.944 Å ($x = 0.5$), in good agreement with the experimental data, 6.046 Å ($x = 0$) [20] and 5.973 Å ($x = 0.44$) [8]. The simulated spin-integrated photoelectron spectra shown in Fig. 2(b), which are obtained by broadening the calculated DOS data using a Gaussian function with a FWHM of 240 meV, reproduce the experimental results reasonably well.

Figure 3(a) shows the valence-band DOS calculated for the cubic phase of $Ni_2Mn_{1+x}Sn_{1-x}$ ($x = 0$, 0.25, and 0.5). A peak structure is found at about 0.51 eV below $E_F$ in the minority-spin band of $Ni_2MnSn$. The peak in the DOS is predominantly composed of Ni $3d$ $e_g$ ($x^2 - y^2$ and $3z^2 - r^2$) orbitals, as pointed out for $Ni_2MnGa$ by several authors [18,27–29]. With an increase in the Mn composition, the peak structure is broadened and shifts towards $E_F$. The peak shift found in the DOS is consistent with the observed spectra in Fig. 2(a). The peak shift can be attributed to the hybridization between the Ni $3d$ orbitals and the $3d$ orbitals of excess Mn atoms at Sn sites. It should be noted that the magnetic moment of excess Mn at the Sn sites (denoted by "$Mn_{Sn}$" hereafter) is antiparallel to that of Mn at the ordinary sites. Thus, the occupied $Mn_{Sn}$ $3d$ states are located on the lower energy (or higher binding energy) side of the Ni $3d$ states in the minority-spin band. Then, the hybridization between the $Mn_{Sn}$ $3d$ and the Ni $3d$ orbitals causes the energy shift of the Ni $3d$ bands towards $E_F$. The antiferromagnetic coupling between the excess Mn and the ordinary Mn magnetic moments has also been predicted theoretically for Ni-Mn-Ga alloys [30]. The antiparallel arrangement of the Mn magnetic moment causes the decrease of the net magnetization from $4.09\mu_B$ per formula ($x = 0$) to $1.92\mu_B$ per formula ($x = 0.5$), which agrees with a previous magnetization measurement [19].

We have also calculated the total-energy variation caused by a tetragonal distortion from the cubic phase, while fixing the cell volume at that of the cubic phase for each Mn composition. The results are shown in Fig. 3(b). The cubic phase is energetically favorable for stoichiometric $Ni_2MnSn$, as reported previously [28]. Interestingly, the

cubic phase tends to be unstable against the tetragonal distortion with increasing Mn composition. For $Ni_2Mn_{1.5}Sn_{0.5}$ ($x = 0.5$), two minima in the total energy are located at $c/a = 0.94$ and 1.31, respectively, and the latter is energetically favorable. The theoretical results are consistent with the experimental observation that the MPT takes place for $x \geq 0.36$ in $Ni_2Mn_{1+x}Sn_{1-x}$ with $c/a > 1$ [5,31]. The instability of the cubic phase for higher Mn compositions is closely related to the electronic structure variation with increasing excess Mn composition. In the tetragonal structure, the degenerate Ni $3d$ $e_g$ level splits into two levels; one, on the higher energy side, is composed of the $x^2 - y^2$ orbital, and the other, on the lower energy side, the $3z^2 - r^2$ orbital, for $c/a > 1$. This band splitting decreases the total energy, thereby stabilizing the lattice distortion due to the so-called Jahn-Teller effect. A noticeable energy stabilization is expected when $E_F$ is located in between the two split-off levels, as in the case of $Ni_2Mn_{1.5}Sn_{0.5}$ ($x = 0.5$). The simulated spectra in Fig. 2(b) for the tetragonal phase ($x = 0.5$) reproduced well the disappearance of the peak structure below the MPT temperature seen in Figs. 1(a) and 1(b). On the other hand, only a subtle energy stabilization is expected when both the split-off levels are completely occupied by electrons, as in the case of $Ni_2MnSn$ ($x = 0$). This is the reason why the martensite phase is stabilized only for Ni-Mn-Sn alloys having larger amounts of excess Mn atoms.

In summary, we have investigated the temperature dependence of the electronic structures of $Ni_2Mn_{1+x}Sn_{1-x}$ by means of bulk sensitive hard-x-ray photoelectron spectroscopy and *ab initio* calculation. The peak structure composed of the minority-spin $3d$ $e_g$ states in the high temperature cubic phase shows a systematic energy shift towards $E_F$ with increasing $x$. According to the first-principles calculation, the peak shift is attributable to the hybridization between the Ni $3d$ $e_g$ states and the $3d$ states of excess Mn atoms at Sn sites, which are antiferromagnetically coupled. For $x \geq 0.36$, we have probed the change of electronic structure due to the MPT. The Jahn-Teller splitting of the Ni $3d$ $e_g$ states plays an important role in driving the instability of the cubic phase for $x \geq 0.36$. These findings gain deeper insight into the microscopic driving force of MPTs in Ni-Mn-Sn and the related ferromagnetic shape memory alloys.

The experiments were performed at BL15XU of SPring-8 with the approval of NIMS Beamline Station (Proposal No. 2009A4800). We acknowledge Y. Yamashita and H. Yoshikawa of NIMS for their technical support during the experiment. We also acknowledge Mr. K. Obara of IMR, Tohoku University, for sample preparation. This work was partially supported by a Grant-in-Aid for Scientific Research (Grants No. 17340112, No. 19048002, and No. 21560693) from JSPS/MEXT and by a Cooperative Research Project of RIEC, Tohoku University.

*akiok@hiroshima-u.ac.jp

[1] P. J. Webster *et al.*, Philos. Mag. B **49**, 295 (1984).
[2] K. Ullakko *et al.*, Appl. Phys. Lett. **69**, 1966 (1996).
[3] A. N. Vasil'ev *et al.*, Usp. Fiz. Nauk **173**, 577 (2003) [Phys. Usp. **46**, 559 (2003)].
[4] P. Entel *et al.*, J. Phys. D **39**, 865 (2006).
[5] Y. Sutou *et al.*, Appl. Phys. Lett. **85**, 4358 (2004).
[6] R. Kainuma *et al.*, Nature (London) **439**, 957 (2006).
[7] A. Planes, L. Manosa, and M. Acet, J. Phys. Condens. Matter **21**, 233201 (2009).
[8] T. Krenke *et al.*, Nature Mater. **4**, 450 (2005).
[9] S. Y. Yu *et al.*, Appl. Phys. Lett. **89**, 162503 (2006).
[10] B. Zhang *et al.*, Appl. Phys. Lett. **91**, 012510 (2007).
[11] M. Khan *et al.*, Appl. Phys. Lett. **91**, 072510 (2007).
[12] P. J. Brown *et al.*, J. Phys. Condens. Matter **18**, 2249 (2006).
[13] R. Y. Umetsu *et al.*, Appl. Phys. Lett. **93**, 042509 (2008).
[14] S. Aksoy *et al.*, Phys. Rev. B **79**, 212401 (2009).
[15] K. Koyama *et al.*, Appl. Phys. Lett. **89**, 182510 (2006).
[16] K. Koyama *et al.*, J. Magn. Magn. Mater. **310**, e994 (2007).
[17] S. Fujii, S. Ishida, and S. Asano, J. Phys. Soc. Jpn. **58**, 3657 (1989).
[18] C. P. Opeil *et al.*, Phys. Rev. Lett. **100**, 165703 (2008).
[19] T. Kanomata *et al.*, Mater. Sci. Forum **583**, 119 (2008).
[20] T. Krenke *et al.*, Phys. Rev. B **72**, 014412 (2005).
[21] K. Kobayshi *et al.*, Appl. Phys. Lett. **83**, 1005 (2003).
[22] G. Kresse and J. Hafner, Phys. Rev. B **47**, 558 (1993).
[23] G. Kresse and J. Furthmüller, Comput. Mater. Sci. **6**, 15 (1996); Phys. Rev. B **54**, 11 169 (1996).
[24] J. P. Perdew, K. Burke, and M. Ernzerhof, Phys. Rev. Lett. **77**, 3865 (1996).
[25] P. E. Blöchl, Phys. Rev. B **50**, 17 953 (1994).
[26] G. Kresse and D. Joubert, Phys. Rev. B **59**, 1758 (1999).
[27] S. R. Barman, S. Banik, and A. Chakrabarti, Phys. Rev. B **72**, 184410 (2005).
[28] A. Ayuela *et al.*, J. Phys. Condens. Matter **11**, 2017 (1999).
[29] A. Ayuela, J. Enkovaara, and R. M. Nieminen, J. Phys. Condens. Matter **14**, 5325 (2002).
[30] J. Enkovaara *et al.*, Phys. Rev. B **67**, 212405 (2003).
[31] The present layered $4O$-type structure can be approximately considered as the distorted $L2_1$ phase (denoted as a face-centered tetragonal structure) with a high density of ordered nanotwins [A. G. Khachaturyan, S. M. Shapiro, and S. Semenovskaya, Phys. Rev. B **43**, 10 832 (1991)]. In the $Ni_2Mn_{1.44}Sn_{0.44}$ alloy, the lattice parameters for the distorted $L2_1$ phase can be evaluated as being $c/a = 1.1938$.